STUDIA UNIVERSITATIS BABEŞ-BOLYAI
Engineering 70(1) 2025 DOI: 10.24193/subbeng.2025.3

Influence of Infill Density on Dimensional and Geometrical Deviations of PLA Parts Fabricated by FDM

Raul-Rusalin Turiac, Zoltan-Iosif Korka*, Alexandra-Teodora Aman, Mihael Magda

Abstract. *The study investigates the influence of infill density on the dimensional and geometric deviations of Polylactic Acid (PLA) cubic specimens manufactured using Fused Deposition Modeling (FDM). Five infill levels (20–100%) were analyzed, while all other process parameters were kept constant. Flatness, parallelism, perpendicularity, and dimensional measurements were performed using a Mitutoyo MiSTAR 555 coordinate measuring machine, providing micron-level accuracy. The results show that infill density has selective and direction-dependent effects on geometric accuracy, without indicating a general trend applicable to all types of deviations. A linear increase in printing time and specimen mass was also observed as infill density increased, indicating a direct impact on manufacturing cost.*

Keywords*: Fused Deposition Modeling (FDM), Polylactic Acid (PLA), Infill Density, Dimensional Accuracy, Geometrical Deviations*

1. Introduction

Three-dimensional printing using Fused Deposition Modeling (FDM) has advanced significantly in recent years, becoming one of the most widely used methods for the rapid fabrication of prototypes and functional polymer components. The technology operates by the controlled extrusion of a heated thermoplastic filament, which is deposited layer by layer according to a previously generated digital model. The simplicity of the process, the relatively low equipment cost, and the ability to produce complex geometries have contributed decisively to its widespread adoption in industrial, educational, and research environments.

However, the layer-by-layer nature of FDM parts introduces variability that can affect surface quality, dimensional accuracy, and the mechanical behavior of the final products. In practice, parts manufactured via FDM may exhibit deviations from their designed dimensions, phenomena often associated with the ways in which process parameters influence the deposition of the molten material. Parameters such as printing speed, filament color, layer thickness, or printing strategy [1-3] are only a few of the factors that determine the dimensional stability of components produced by this technology.

Although the literature addresses a wide range of process parameters, the density and pattern of the infill remain comparatively less explored than variables such as temperature, speed, or printing orientation. The infill represents the internal structure of the part and can be configured in various geometric patterns (rectilinear, concentric, honeycomb, HilbertCurve, and others), each distributing material differently throughout the volume and influencing both internal stiffness and the way the part stabilizes dimensionally.

In their study, Khan et al. [4] analyzed the tensile and flexural behavior of PLA specimens with different infill patterns and observed that the rectilinear structure generated the highest values of strength and elastic modulus (19.1 MPa and E = 10.51 GPa in tension; 24.4 MPa and E= 0.359 GPa in flexure), whereas the HilbertCurve pattern resulted in the lowest mechanical performance.

Infill density is another parameter that directly influences the mechanical behavior of FDM-manufactured parts due to its role in the internal distribution of material and in the way, loads are transmitted throughout the structure. Abdulridha et al. [5] highlight the essential importance of this parameter, showing that infill density exhibits the highest statistical significance on the compressive strength of PLA specimens, with values increasing from approximately 4 MPa to 56.5 MPa as the density is raised from 20% to 100%.

Similarly, various research studies conclude that denser internal structures reduce porosity, improve interlayer cohesion, and provide superior mechanical performance. The results reported in recent research consistently indicate that high infill density leads to increases in stiffness, tensile strength, and elastic modulus, regardless of the infill pattern used [6-10].

For applications, in which geometric accuracy is critical, understanding how infill density alters material distribution and the shrinkage or post-deposition stabilization processes, becomes essential. In the specialized literature, several studies confirm that infill influences the dimensional deviations of PLA parts. Alafaghani et al. [11] report that infill percentage is among the most influential parameters affecting dimensional accuracy: low values (20%) generate the smallest cumulative errors, whereas 100% infill leads to oversizing due to excessive material accumulation. Similarly, Abas et al. [12] report increases in deviations as density is raised from 20% to 50%, the deviation in length increases from ~0.4% to 0.9%, in width from ~1.1% to 2.0%, and in height from ~1.0% to 1.3%, with deformations confirmed microscopically. Comparable results are presented by Zonoobi et al. [13], where densities of 10%, 30%, and 50%

show that infill is the second most influential factor affecting dimensional errors (after layer thickness), with the smallest deviations obtained at 10% infill and the largest at 50%. Solouki et al. [14] confirm the same moderate trend: increasing infill from 60% to 80% leads to slight increases in deviations (length: 0.75–0.78 mm; width: 0.31–0.35 mm), depth deviation although decreases (0.015–0.01 mm).

However, certain studies identify the presence of optimal infill levels. Singh et al. [15] observe that dimensional accuracy is highest at 40% infill; higher values (60–80%) generate internal stresses and amplify deviations. Similarly, Galetto et al. [16], analyzing the 5–20% range, show that intermediate values (13–19%) provide the best dimensional accuracy, without revealing a global monotonic trend. Gunes et al. [17] confirm that the effect of infill density is not systematic, with variations depending on part geometry: each shape exhibits its own optimal density range for minimizing deviations. In a broader analysis covering 10–100%, Vălean et al. [18] report very small deviations (below 0.14%), with the lowest errors at 90% infill, while low-density levels (10–30%) show the highest variability. Miron et al. [18], analyzing densities between 20–100%, identify a maximum error of ~0.9% in specimen width, which tends to decrease as infill increases, whereas deviations in length and thickness do not follow a clear trend.

Overall, the literature shows that infill density can influence dimensional accuracy; however, the conclusions are inconsistent, primarily because most studies simultaneously modify multiple process parameters (layer height, orientation, speed, temperature, infill pattern), making it difficult to isolate the specific effect of infill density. Furthermore, some studies do not fully report experimental conditions, part geometry, or measurement methods, limiting the formulation of a universally valid relationship between infill and dimensional deviations.

In this context, the present study aims to directly investigate the influence of infill density on the dimensional deviations of PLA parts manufactured via FDM, varying exclusively this parameter throughout the experiment. The novelty of the study lies not only in isolating the effect of infill density but also in the depth of the analysis: dimensional deviations are evaluated using high-precision metrological equipment capable of detecting micron-level variations, allowing for a much more accurate characterization of geometric behavior. In addition, essential components of part performance (surface flatness, parallelism, and perpendicularity) are analyzed alongside the influence of infill density on printing time and material consumption, factors highly relevant for optimizing manufacturing costs.

2. Materials and Methods

To examine the influence of infill density on dimensional deviations, a batch of 25 cubic test samples (5 specimens for each infill density of 20, 40, 60, 80 and 100%) was manufactured using FDM technology. The geometry of the samples and their nominal dimensions are presented in Figure 1.

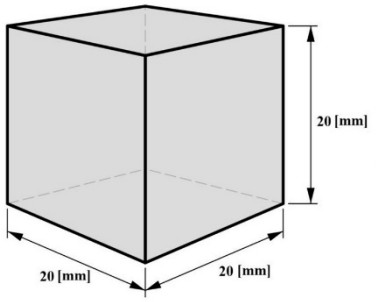

Figure 1. Geometry of the cubic test specimen and its nominal dimensions

2.1. Printing of the Test Specimens

The test specimens were printed on a Creality Ender-3 V3 KE printer using Polymaker PLA Panchroma filament in satin black. The process parameters were kept constant throughout the fabrication of the entire batch, with their values listed in Table 1. The only experimental variable was the infill density, for which five levels were selected. Five specimens were manufactured for each level to achieve the highest possible measurement accuracy.

Table 1. Process parameters used for printing the test specimens

Material	PLA
Filament diameter	1.75 mm
Nozzle diameter	0.4 mm
Extruder temperature	210 °C
Printing bed temperature	60 °C
Layer thickness	0.20 mm
Printing speed	50 mm/s
Fan	Yes, at 50% of the maximum power
Orientation	YX
Infill raster angle	0°/90°
Infill density	20 / 40 / 60 / 80 / 100 %
Infill pattern	Gyroid
Number of contour lines	2
Top layers	4
Bottom layers	4
Top/Bottom pattern	Zig Zag
Top/Bottom raster angle	45°/135°

In the case of the gyroid infill pattern, the internal structure is generated parametrically by the slicer as a triply periodic minimal surface (TPMS). Consequently, the raster angle parameter does not significantly alter the internal geometry in the same manner as in linear or grid infill patterns, where strand orientation directly governs structural anisotropy.

To illustrate the variation of the internal structure as a function of infill density, Figure 2 shows the slicer-generated renderings (Creality Print) for layer 50 of the specimens, selected as an intermediate level from the total of 100 layers that form the final geometry.

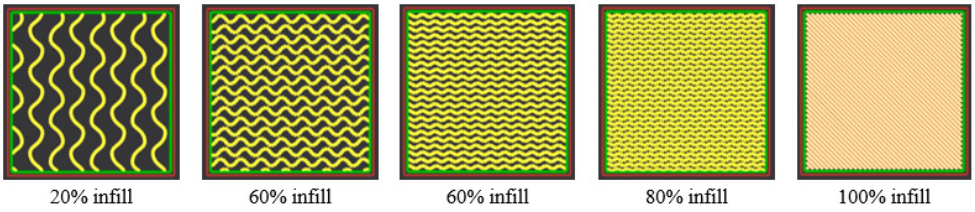

Figure 2. Internal structure at layer 50 for different infill densities

It should be noted that at 100% infill density, the slicing software generates a fully solid structure, and the selected infill pattern no longer governs the internal geometry. In this case, the internal region is filled using the same configuration as the solid top and bottom layers, namely a Zig Zag pattern with a raster angle of 45°/135°. This behavior results from the slicer's default solid-fill strategy rather than from a modification of the experimental parameters.

2.2. Dimensional Measurements

To identify the influence of infill density on the PLA specimens, both dimensional measurements along the three principal directions of the cubic samples and geometric form deviations were performed. These included the deviations from flatness for all cube faces, the parallelism deviations between opposite faces, and the perpendicularity deviation between all adjacent faces.

The measurements were carried out using a Mitutoyo MiSTAR 555 Coordinate Measuring Machine (CMM), equipped with a Renishaw SP25M scanning probe and SM25-1 module, fitted with a ruby-tipped stylus of size M3 fixture, length 31 mm and 4 mm ball diameter. Data acquisition and measurement processing were performed using the CAT1000 and GEOPAK software modules. The equipment used is illustrated in Figures 3(a) and 3(b).

a b

Figure 3. Mitutoyo MiSTAR 555 coordinate measuring machine and specimen setup for dimensional measurements

Both the point-measurement function and the probing scan mode were used for the dimensional measurements to obtain superior accuracy. As shown in Figure 3(b), the method of fixture positioning limits the probe's access to the lower face of the cube. Consequently, to avoid errors caused by restricted accessibility and to maintain measurement precision, the base of the part was analyzed using two distinct planes, determined in separate positions.

Figure 4 presents an example of a report generated by the coordinate measuring machine, including the measurement paths, evaluated surfaces, and the deviation values determined for flatness, parallelism, and perpendicularity. The software representation illustrates how the measurement points were acquired and the distribution of deviations across the analyzed surfaces.

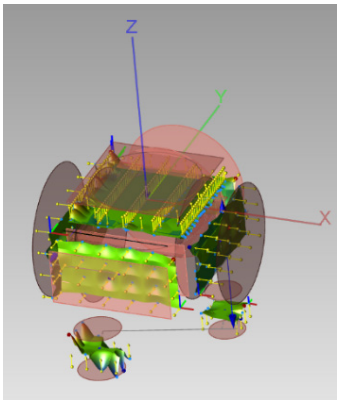

Figure 4. Example of a CMM report showing measurement paths, evaluated surfaces, and the distribution of flatness, parallelism, and perpendicularity deviations

In the graphical analyses presented in the results section, the mean values obtained from the five measurements performed on each of the five specimens corresponding to each infill density level were used. For a consistent interpretation of the data, Figure 5 presents the notation convention for the six analyzed planes:

A – front plane
B – top plane
C – right-side plane
D – left-side plane
E – bottom plane
F – rear plane

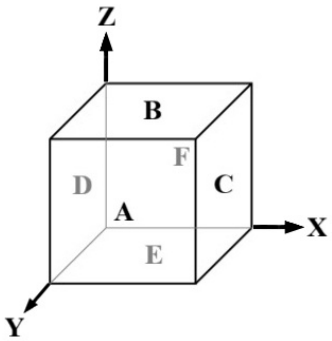

Figure 5. Notation convention for the six planes of the cubic test specimen

The X, Y, and Z axes illustrated in Figure 5 define the reference system of the specimen in its printing orientation. All specimens were measured while maintaining the same orientation as during fabrication, without reorientation relative to the coordinate measuring machine, in order to preserve the direct correspondence between printing directions and the measured dimensional deviations.

The measurements were carried out in the laboratory at 20 ± 1 °C, in accordance with the conditions recommended by the equipment manufacturer.

3. Results and Discussions

3.1. Dimensional Deviations

The dimensional deviations were automatically generated by the measurement software based on the values acquired by the CMM. Figure 6 (a–c) presents the mean deviations determined for the three analyzed pairs of planes (B–E, C–D, and A–F), which are relevant for the cubic geometry of the specimens.

For all pairs of planes, the deviations are negative, indicating a slight overall undersizing of the parts. However, the values are small, ranging from (–9.6 μm) to (–133 μm), which confirms good reproducibility of the FDM process for the analyzed geometry.

B–E distance (specimen height) – figure 6 a

The deviations are the smallest among all three measured directions. The maximum deviation, –41.4 μm, was recorded at 60% infill, while the minimum deviation, –9.6 μm, occurred at 40% infill. No clear trend correlated with infill density was observed. This high stability along the vertical (Z) direction can be explained by the fact that the part height is directly controlled by the layer-by-layer deposition increment, which limits the lateral flow of the molten material, an effect that is more pronounced along the X and Y directions.

C–D distance – figure 6 b

The values are larger than those along the B–E axis, ranging from –70.6 μm (80% infill) to –125.6 μm (60% infill). As in the case of the B–E distance, no coherent trend of the deviations as a function of infill density can be identified. The fluctuations can be explained by non-uniform shrinkage during cooling and by variations in internal stiffness provided by the infill structure.

A–F distance – figure 6 c

This direction exhibits the most noticeable trend. The deviation values decrease gradually with increasing infill density, from –133 μm at 20% infill to –102.3 μm at 80% infill. The observed improvement results from the progressive structural stiffening of the specimens, which reduces deformation along the longitudinal direction. At 100% infill, a slight increase in deviation is observed, suggesting that increasing density does not guarantee continuous improvement, phenomenon also reported in the literature.

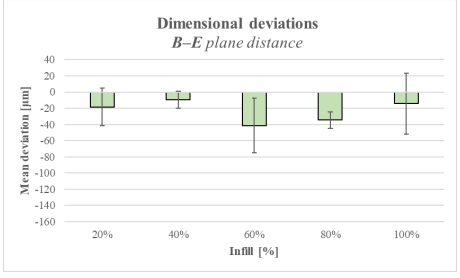

a

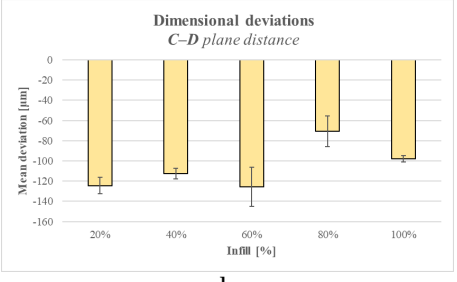

b

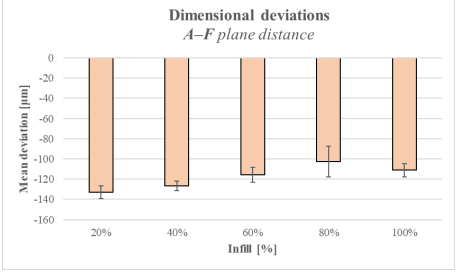

c

Figure 6. Mean dimensional deviations as a function of infill density

Overall, the dimensional deviations reveal different behaviors along the three analyzed directions. The deviations along the Z direction (B–E distance) are consistently the smallest, confirming the much stricter control of height in the FDM process, due to the layer-by-layer deposition and the absence of lateral material flow. In contrast, the horizontal directions (C–D and A–F) exhibit larger deviations, influenced by material shrinkage and the variable internal stiffness determined by the infill density. The only clear trend is observed along the Y direction (A–F distance), where increasing infill density leads, up to a certain point, to a reduction of deviations. Nevertheless, the behavior across the three axes suggests that the influence of infill density on dimensional accuracy is not uniform, depending significantly on the analyzed direction and on the way the material stabilizes during the cooling process.

3.2. Flatness Deviations

Figure 7 presents the flatness deviations for all six planes of the analyzed specimens. Overall, the values are low, not exceeding 90 μm, which indicates good geometric stability of the FDM-printed samples.

Planes A, C, and F exhibit a progressive increase in deviations as the infill density increases, reaching their maximum values at 80% infill, followed by a decrease at 100% infill. The minimum values are consistently recorded at 20% infill. This nonlinear evolution indicates that the relationship between infill density and flatness deviation is not monotonic. The increase in deviations up to 80% infill followed by a reduction at 100% may be influenced by the structural transition from a gyroid-filled configuration to a fully solid structure. This change may alter the overall stiffness and the redistribution of thermal and residual stresses within the part. However, internal stresses were not directly quantified in the present study, and therefore no specific causal mechanism is asserted.

Plane D, which contains the highest deviation in the entire dataset (87.6 μm at 80% infill), follows a similar pattern; although the variation is more pronounced. For this plane, the minimum deviation of 41.4 μm was recorded at 100% infill, confirming the trend toward geometric stabilization at very high densities.

Plane E shows a predominantly increasing behavior; however, the specimens at 40% infill deviate from this trend, exhibiting a higher value than those in the intermediate range. Even so, the maximum deviation is reached at 100% infill and the minimum at 20% infill, indicating a general correlation between increasing infill density and the intensification of stresses that affect flatness.

Plane B, the top surface of the specimen, does not exhibit a coherent variation with respect to infill density. The absence of a trend can be attributed to the fact that surface B represents the last deposited layer, which, typical of the FDM process, exhibits increased roughness and heightened sensitivity to the cooling and deposition features of the extruder.

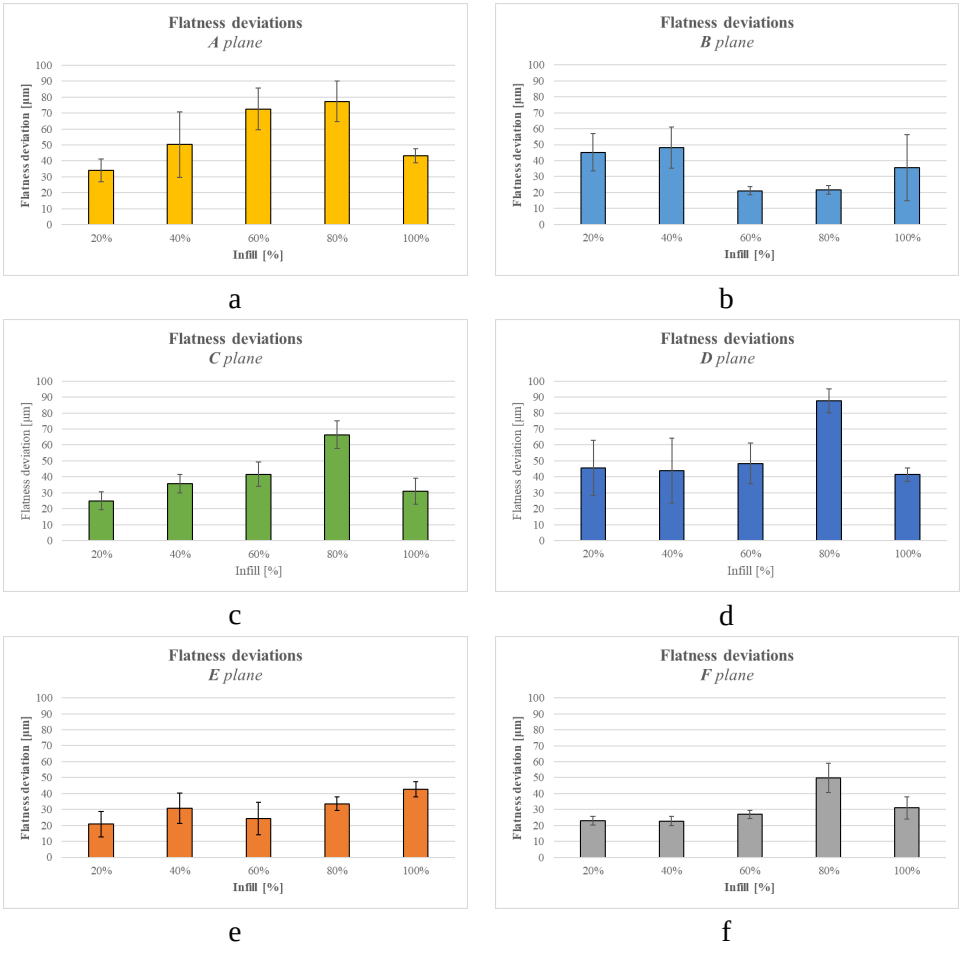

Figure 7. Influence of infill density on flatness deviations

Overall, the flatness deviations remain within low limits, yet clear tendencies can be observed on most planes: increasing infill density leads, up to a threshold of approximately 80%, to amplified deviations, followed by slight stabilization at 100% infill. The exceptions recorded on plane B and at certain intermediate levels (such as 40% infill on plane E) confirm that both local geometry and the sequence of deposited layers influence the way internal stresses affect surface flatness.

3.3. Parallelism Deviations

Figure 8 presents the parallelism deviations for the three pairs of planes of the analyzed specimens. Overall, the values are low, not exceeding 118.8 μm (B–E planes at 100% infill), which indicates good geometric stability of the FDM-printed parts.

For the A–F and C–D planes, a coherent evolution of the deviations is observed: they increase progressively with the infill density, reach a maximum at 80% infill, and subsequently decrease at 100% infill. The minimum deviations are consistently recorded at 20% infill, and the maximum deviations at 80% infill. This variation suggests that the internal stiffening induced by high infill densities may accentuate local deformations up to a certain threshold, followed by structural stabilization under full infill conditions.

In contrast, the parallelism of planes B–E (the upper and lower surfaces of the specimen) does not follow a clear trend with respect to infill density, with parallelism deviations reaching a maximum of 118.8 μm at 100% infill. When these results are correlated with the deviations of the B–E plane distance analyzed previously (which did not exceed a maximum value of –41.4 μm), it can be observed that global dimensional stability along the Z direction does not necessarily imply a similar evolution of parallelism.

This difference can be explained by the distinct geometric nature of the two quantities: the distance between planes represents an average dimensional deviation, whereas parallelism is sensitive to local variations in form and orientation. The upper plane (B), corresponding to the final deposited layer, exhibits increased roughness characteristic of the FDM process, while the lower plane (E), which is in contact with the build plate, is influenced by adhesion conditions and the surface characteristics of the plate.

Furthermore, as described in Section 2.2, the lower plane was determined as the mean of two separate plane evaluations performed in distinct positions imposed by fixture constraints, which may contribute to additional variability in the parallelism results.

Overall, the parallelism deviations remain low, with a clear evolution along the A–F and C–D directions, where increasing infill density leads to intensified deviations up to a maximum at 80% infill, followed by stabilization at 100%. The B–E planes do not exhibit a clear dependence on infill density, reflecting the strong influence of deposition characteristics on the upper plane and build-plate interaction on the lower plane—factors that attenuate the effect of internal stiffening.

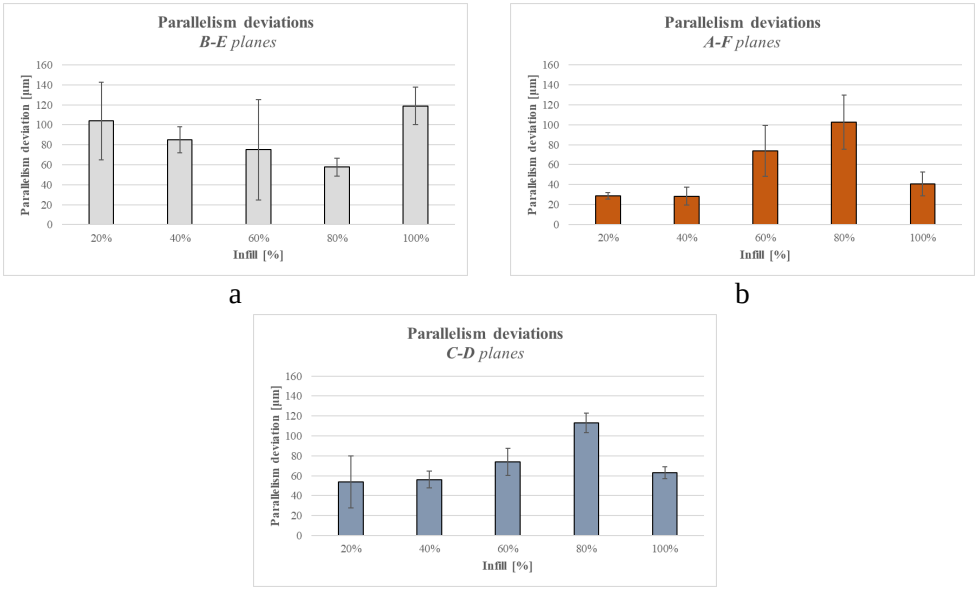

Figure 8. Parallelism deviations for the three analyzed plane pairs

3.4. Perpendicularity Deviations

Figure 9 presents the perpendicularity deviations for all analyzed plane pairs. Overall, the values are moderate, with a maximum of 228.8 µm for the perpendicularity of planes B–C at 20% infill, which also represents the largest deviation recorded in this measurement set.

However, the behavior of the deviations varies depending on the plane pair. For the B–F and F–D planes, the deviations increase with infill density, reaching a maximum at 80% infill and decreasing subsequently at 100% infill. The minimum values occur at 20% infill, suggesting that the progressive stiffening of the internal structure accentuates deviations up to a certain threshold, followed by geometric stabilization under full infill conditions.

The perpendicularities of the D–A, C–A, and F–C planes exhibit a similar trend, with an almost constant increase in deviations (though with local variations around 40% infill), the maxima being recorded at 80% infill, except for the F–C pair, where the maximum deviation occurs at 40% infill. At 100% infill, all these cases show a reduction in deviations.

For the E–F and E–D plane pairs, the deviations increase steadily with infill density, with the highest values reached at 100% infill and the lowest at 20%. This evolution indicates that the stiffening of the internal volume directly affects the maintenance of perpendicularity between planes, without stabilization at high infill levels.

Conversely, the perpendicularities of the B–C and D–B planes show an overall decreasing trend as infill increases, although the values obtained at 20% and 100% infill deviate from this evolution and stand out compared to the intermediate levels. These discrepancies can be explained by the increased sensitivity of these planes to variations in cooling and shrinkage, influenced both by internal stiffness and by the sequence of deposited layers.

For the B–A and E–C plane pairs, no clear correlation between infill density and perpendicularity deviations is observed. Both pairs include either the top or bottom plane of the specimen, surfaces that are inherently more sensitive to variations in the FDM process. The top plane corresponds to the final deposited layer, characterized by high roughness and low thermal stability, while the bottom plane is influenced by the contact conditions with the build plate, factors that can override the effect of infill density.

Overall, the perpendicularity deviations fall within moderate ranges but exhibit noticeable variations depending on the analyzed plane pair. Most pairs show an increase in deviations with rising infill density up to 60–80%, followed by a reduction at 100%, indicating a balance between internal stiffening and geometric stabilization. However, certain plane pairs, particularly those including the top or bottom surfaces of the part, do not follow a clear trend, being strongly influenced by FDM process-specific characteristics and the layer-by-layer deposition phenomenon.

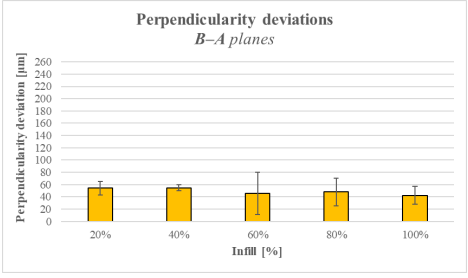

a

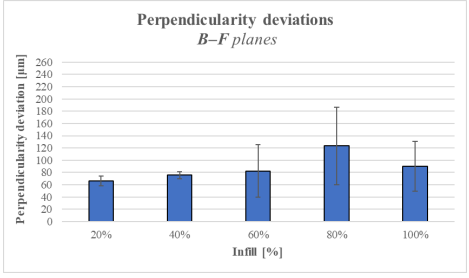

b

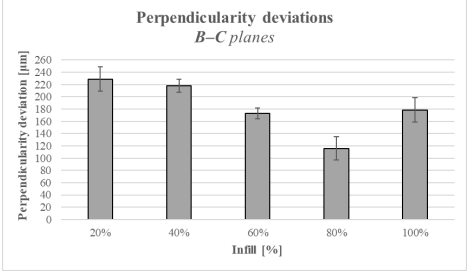

c

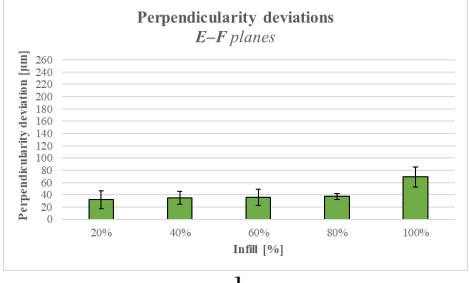

d

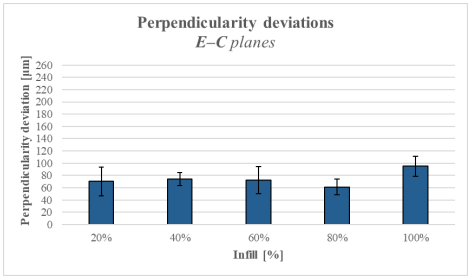

e

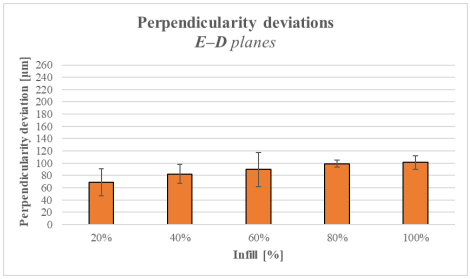

f

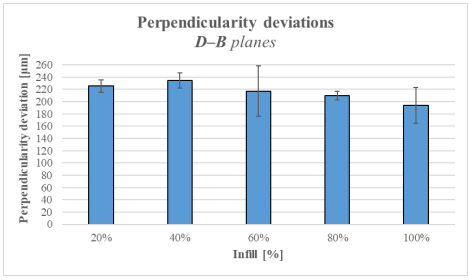

g

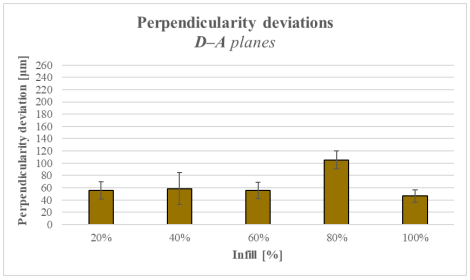

h

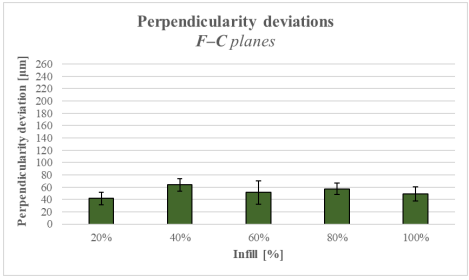

i

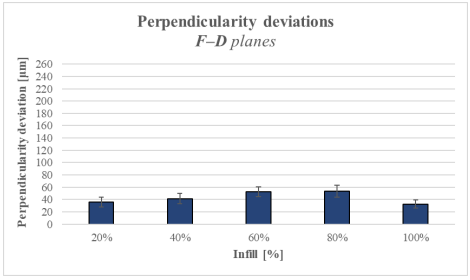

j

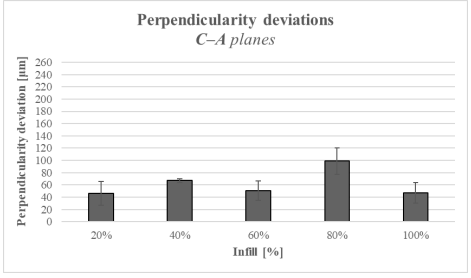

k

Figure 9. Perpendicularity deviations for the analyzed plane pairs

3.5. Variation of Mass and Printing Time

The influence of infill density is reflected not only in geometric deviations but also in production costs, since both the mass of material used and the required printing time are directly dependent on the amount of material deposited inside the part. The data regarding printing time and estimated material mass were collected from the Creality Print software used to generate the G-code for each specimen. Figures 10a and 10b present the variation of mass and printing time as a function of infill density.

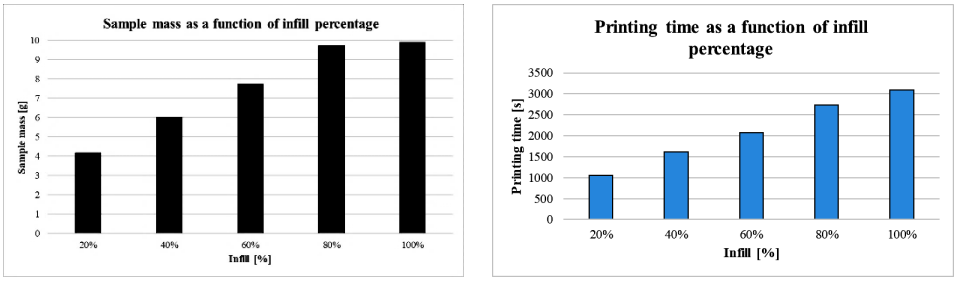

a b

Figure 10. Influence of infill density on specimen mass and printing time

A linear increase in specimen mass is observed, from 4.17 g at 20% infill to 9.86 g at 100% infill. This evolution is expected, given that the infill corresponds to the internal volume of the part, and increasing its density directly results in a larger amount of extruded material.

The printing time follows the same trend, increasing from 1060 s at 20% infill to 3089 s at 100% infill. As the infill density increases, the extruder must follow a larger number of internal paths, which extends the printing time and, consequently, the energy consumption of the process.

These results highlight that the choice of infill density has a direct impact on the overall production cost. A high infill density provides superior internal stiffening but requires both increased material consumption and significantly longer production times. Therefore, the infill level must be selected according to the functional requirements of the part (whether mechanical or geometric) to achieve an optimal compromise between performance, accuracy, and cost.

4. Conclusion

The study analyzed the influence of infill density on the dimensional, flatness, parallelism, and perpendicularity deviations of cubic specimens fabricated using FDM technology, employing five infill levels (20–100%). The obtained results allowed us to formulate the following conclusions:

- Dimensional deviations were negative and remained within relatively small limits (below –140 μm), without showing a clear dependence on infill level for all analyzed directions. Only for the A–F distance was a gradual improvement observed as infill increased up to 80%.
- Flatness deviations exhibited moderate increases for planes A, C, D, and F in the 20–80% infill range, followed by a decrease at 100%. The top (B) and bottom (E) planes showed irregular behavior, most likely due to the characteristic roughness of the final printed layer and the non-uniform adhesion to the build plate, which makes it difficult to identify a general infill-dependent trend.
- Parallelism deviations showed an increasing trend up to 80% infill for the A–F and C–D plane pairs, followed by a decrease at 100%. In contrast, the B–E pair did not show a consistent influence of infill density, suggesting that the top and bottom surfaces are more affected by the deposition characteristics of the final layers than by the internal structure of the part.
- Perpendicularity deviations displayed diverse behaviors without a unified trend. Some plane pairs (B–F, F–D) exhibited progressive increases in deviations up to 80% infill, followed by decreases at 100%, while others (E–F, E–D) showed an almost linear increase across the entire analyzed range. The B–C and D–B pairs showed decreasing deviations as infill increased, but the extreme values at 20% and 100% deviated from the general trend, indicating localized instabilities.
- Printing time and specimen mass increased linearly with infill density, confirming that higher densities involve greater material consumption and longer fabrication times. This trend must be considered when optimizing production costs.

Overall, the results indicate that infill density does not exert a strong or systematic influence on the geometric accuracy of the small-sized parts analyzed in this study. Instead, the observed effects are moderate, selective, and dependent on the orientation of the surfaces.

Given these findings, future research directions will include the fabrication of significantly larger parts, for which the effects of infill density on thermal stability, shrinkage, and geometric distortions may become more pronounced. Additionally, extending the investigation to mechanical testing and incorporating different infill patterns could contribute to the development of clearer predictive models regarding the geometric behavior of PLA in FDM processes.

References

1 Ardeljan D.D., Frunzaverde D., Cojocaru V., Turiac R.R., Băcescu N., Ciubotariu C.R., Mărginian G., The Impact of Elevated Printing Speeds and Filament Color on the Dimensional Precision and Tensile Properties of FDM-Printed PLA Specimens, *Polymers*, 17(15), 2025.

2 Cojocaru V., Turiac R.R., Frunzaverde D., Trișcă G., Băcescu N., Mărginian G., Effect of the Printing Scenario on the Dimensional Accuracy and the Tensile Strength of Different Colored PLA Specimens Produced by Fused Deposition Modeling, *Applied Sciences*, 14(17), 2024.
3 Frunzăverde D., Cojocaru V., Băcescu N., Ciubotariu C.-R., Micloșină C.-O., Turiac R.R., Mărginian G., The Influence of the Layer Height and the Filament Color on the Dimensional Accuracy and the Tensile Strength of FDM-Printed PLA Specimens, *Polymers*, 15(10), 2023.
4 Khan S.F., Zakaria H., Chong Y.L., Saad M.A., Basaruddin K., Effect of Infill on Tensile and Flexural Strength of 3D Printed PLA Parts, *IOP Conference Series: Materials Science and Engineering*, 429, 2018.
5 Abdulridha H., Abbas T., Analyzing the Impact of FDM Parameters on Compression Strength and Dimensional Accuracy in 3D Printed PLA Parts, *Engineering and Technology Journal*, 41(12), 2023, pp. 1611–1626.
6 Dave H.K., Patadiya N.H., Prajapati A.R., Rajpurohit S.R., Effect of Infill Pattern and Infill Density at Varying Part Orientation on Tensile Properties of Fused Deposition Modeling-Printed Poly-Lactic Acid Part, *Proceedings of the Institution of Mechanical Engineers, Part C: Journal of Mechanical Engineering Science*, 235(10), 2019, pp. 1811–1827.
7 Kadhum A.H., Al-Zubaidi S., AlKareem S.S., Optimization of Mechanical Properties and Surface Characteristics of PLA+ 3D Printing Materials, *International Journal of Chemical Engineering*, 2023.
8 Moradi M., Rezayat M., Rozhbiany F.A.R., Meiabadi S., Casalino G., Shamsborhan M., Bijoy A., Chakkingal S., Lawrence M., Mohammed N., Karamimoghadam M., Correlation between Infill Percentages, Layer Width, and Mechanical Properties in Fused Deposition Modelling of Poly-Lactic Acid 3D Printing, *Machines*, 11(10), 2023.
9 Öteyaka M.Ö., Aybar K., Öteyaka H.C., Effect of Infill Ratio on the Tensile and Flexural Properties of Unreinforced and Carbon Fiber-Reinforced Polylactic Acid Manufactured by Fused Deposition Modeling, *Journal of Materials Engineering and Performance*, 30(7), 2021, pp. 5203–5215.
10 Rismalia M., Hidajat S.C., Permana I.G., Hadisujoto B., Muslimin M., Triawan F., Infill Pattern and Density Effects on the Tensile Properties of 3D Printed PLA Material, *Journal of Physics: Conference Series*, 1402(4), 2019.
11 Alafaghani A., Qattawi A., Investigating the Effect of Fused Deposition Modeling Processing Parameters Using Taguchi Design of Experiment Method, *Journal of Manufacturing Processes*, 36, 2018, pp. 164–174.
12 Abas M., Habib T., Noor S., Salah B., Zimon D., Parametric Investigation and Optimization to Study the Effect of Process Parameters on the Dimensional Deviation of Fused Deposition Modeling of 3D Printed Parts, *Polymers*, 14(17), 2022.

13 Zonoobi M.A., Haghshenas Gorgani H., Javaherneshan D., Experimental Investigation and Multi-Objective Optimization of FDM Process Parameters for Mechanical Strength, Dimensional Accuracy, and Cost Using a Hybrid Algorithm, *Scientia Iranica*, 2023.
14 Solouki A., Aliha M.R., Makui A., Choupani N., Seiti H., Analyzing the Effects of Printing Parameters to Minimize the Dimensional Deviation of Polylactic Acid Parts by Applying Three Different Decision-Making Approaches, *Scientific Reports*, 14(1), 2024.
15 Singh T.K., Birru A.K., Singh K.N., Optimizing the Printing Parameters for Dimensional Accuracy of Distal Femur Bone by Using Taguchi's Method, *Journal of Engineering and Applied Science*, 71(1), 2024.
16 Galetto M., Verna E., Genta G., Effect of Process Parameters on Parts Quality and Process Efficiency of Fused Deposition Modeling, *Computers & Industrial Engineering*, 156, 2021.
17 Gunes S., Ulkir O., Kuncan M., Application of Artificial Neural Network to Evaluation of Dimensional Accuracy of 3D-Printed Polylactic Acid Parts, *Journal of Polymer Science*, 62(9), 2024, pp. 1864–1889.
18 Vălean C., Marşavina L., Linul E., Compressive Behavior of Additively Manufactured Lightweight Structures: Infill Density Optimization Based on Energy Absorption Diagrams, *Journal of Materials Research and Technology*, 33, 2024, pp. 4952–4967.
19 Miron I., Vălean C., Linul E., Infill Density Effect on the Flexural Behavior of FFF-Based AM Polylactic Acid Parts, *Materiale Plastice*, 62(3), 2025, pp. 1–9.

Addresses:

· Eng. Raul-Rusalin Turiac, PhD Candidate, Mechanical Engineering Doctoral School, Babes-Bolyai University,
Traian Vuia Square 1–4, 320085 Reșița, Romania
raul.turiac@ubbcluj.ro
· Assoc. Prof. Dr. Eng. Habil. Zoltan-Iosif Korka, Mechanical Engineering Doctoral School, Babes-Bolyai University,
Traian Vuia Square 1–4, 320085 Reșița, Romania
zoltan.korka@ubbcluj.ro
(**corresponding author*)
· Eng. Alexandra-Teodora Aman, PhD Candidate, Mechanical Engineering Doctoral School, Babes-Bolyai University,
Traian Vuia Square 1–4, 320085 Reșița, Romania
alexandra.aman@ubbcluj.ro

· Eng. Mihael Magda, PhD Candidate, Mechanical Engineering
Doctoral School, Babes-Bolyai University,
Traian Vuia Square 1–4, 320085 Reșița, Romania
mihael.magda@ubbcluj.ro